

Detectable environmental effects in GW190521-like black-hole binaries with LISA

Alexandre Toubiana,^{1,2} Laura Sberna,³ Andrea Caputo,^{4,5,6} Giulia Cusin,⁷ Sylvain Marsat,¹ Karan Jani,⁸ Stanislav Babak,^{1,9} Enrico Barausse,^{10,11} Chiara Caprini,¹ Paolo Pani,¹² Alberto Sesana,^{13,14} and Nicola Tamanini¹⁵

¹*APC, AstroParticule et Cosmologie, Université de Paris, CNRS, F-75013 Paris, France*

²*Institut d'Astrophysique de Paris, CNRS & Sorbonne Universités, UMR 7095, 98 bis bd Arago, 75014 Paris, France*

³*Perimeter Institute, 31 Caroline St N, Ontario, Canada*

⁴*Instituto de Fisica Corpuscular, Universidad de Valencia and CSIC, Edificio Institutos Investigacion, Catedratico Jose Beltran 2, Paterna, 46980 Spain*

⁵*School of Physics and Astronomy, Tel-Aviv University, Tel-Aviv 69978, Israel*

⁶*Department of Particle Physics and Astrophysics, Weizmann Institute of Science, Rehovot 7610001, Israel*

⁷*Université de Genève, Département de Physique Théorique and Centre for Astroparticle Physics, 24 quai Ernest-Ansermet, CH-1211 Genève 4, Switzerland*

⁸*Department Physics and Astronomy, Vanderbilt University, 2301 Vanderbilt Place, Nashville, TN, 37235, USA*

⁹*Moscow Institute of Physics and Technology, Dolgoprudny, Moscow region, Russia*

¹⁰*SISSA, Via Bonomea 265, 34136 Trieste, Italy & INFN, Sezione di Trieste*

¹¹*IFPU - Institute for Fundamental Physics of the Universe, Via Beirut 2, 34014 Trieste, Italy*

¹²*Dipartimento di Fisica, "Sapienza" Università di Roma & Sezione INFN Roma1, Piazzale Aldo Moro 5, 00185, Roma, Italy*

¹³*Department of Physics G. Occhialini, University of Milano - Bicocca, Piazza della Scienza 3, 20126 Milano, Italy*

¹⁴*National Institute of Nuclear Physics INFN, Milano - Bicocca, Piazza della Scienza 3, 20126 Milano, Italy*

¹⁵*Max-Planck-Institut für Gravitationsphysik, Albert-Einstein-Institut, Am Mühlenberg 1, 14476 Potsdam-Golm, Germany.*

GW190521 is the compact binary with the largest masses observed to date, with at least one black hole in the pair-instability gap. This event has also been claimed to be associated with an optical flare observed by the Zwicky Transient Facility in an Active Galactic Nucleus (AGN), possibly due to the post-merger motion of the merger remnant in the AGN gaseous disk. The Laser Interferometer Space Antenna (LISA) may detect up to ten of such gas-rich black hole binaries months to years before their detection by LIGO/Virgo-like interferometers, localizing them in the sky within $\approx 1 \text{ deg}^2$. LISA will also measure directly deviations from purely vacuum and stationary waveforms, arising from gas accretion, dynamical friction, and orbital motion around the AGN's massive black hole (acceleration, strong lensing, and Doppler modulation). LISA will therefore be crucial to alert and point electromagnetic telescopes ahead of time on this novel class of gas-rich sources, to gain direct insight on their physics, and to disentangle environmental effects from corrections to General Relativity that may also appear in the waveforms at low frequencies.

GW190521 is the most massive compact binary merger observed by the LIGO/Virgo Collaboration (LVC), with progenitor black-hole (BH) masses of $85_{-14}^{+21} M_{\odot}$ and $66_{-18}^{+17} M_{\odot}$ [1, 2]. The larger BH lies in the pair-instability gap $\sim [50, 130] M_{\odot}$ [3–5], calling for interpretations beyond standard stellar-evolution models. A viable channel to produce such massive BHs is via repeated mergers (which would also explain the large misaligned spins of GW190521 [1, 2]), e.g. in stellar clusters [6–8] or active galactic nuclei (AGNs) [9–11]. While repeated mergers might be rare in globular clusters, due to BH ejection by gravitational recoil [2], nuclear star clusters have higher escape velocities and more efficiently retain merger remnants. Alternatively, GW190521 may have formed in an AGN disk, where mass segregation and dynamical friction (DF) favor BH accumulation near the center (enhancing merger rates) and their growth by mergers and accretion [9–13]. The large GW190521 masses may also be consistent with metal-free, population-III star progenitors [14] (see also [15–17]). Other less standard scenarios include beyond-Standard-Model physics [18], primordial BHs [19], boson stars [20], and extensions of General Relativity (GR) [21]. Finally, [22, 23] note that there is a non-negligible probability of GW190521 being a “straddling” binary, with components below and above the pair-instability gap. Although some analyses [24–

26] suggest that eccentric waveforms might fit the data better, supporting a dynamical origin in dense environments, the formation of GW190521 remains mysterious.

Remarkably, the Zwicky Transient Facility observed an optical flare (ZTF19abanrhr), interpreted as coming from the kicked GW190521 BH merger remnant moving in an AGN disk [27]. If confirmed, this would be the first electromagnetic counterpart to a BH coalescence (see, however, [28, 29]). The flare occurred ~ 34 days after GW190521 (the delay being ascribed to the remnant's recoil) in AGN J124942.3+344929 at redshift $z = 0.438$. If the flare is indeed associated with GW190521 and due to the remnant's recoil in the AGN disk, [27] finds a total binary mass $\sim 150 M_{\odot}$, kick velocity $\sim 200 \text{ km/s}$ at $\sim 60 \text{ deg}$ from the disk's midplane, a disk aspect ratio (height to galactocentric radius) of $H/a \sim 0.01$, and a gas density of $\rho \sim 10^{-10} \text{ g/cm}^3$. The [27] authors also argue that the binary is most likely located in a disk migration trap (galactocentric distance $a \sim 700 GM/c^2$, with $M \sim 10^8 - 10^9 M_{\odot}$ the mass of the AGN's BH), where gas torques vanish and binaries accumulate as they migrate inward [30]. While the GW190521–ZTF19abanrhr association is debated [31], our results will not rely on it, but only assume that GW190521-like systems reside in gas-rich environments (e.g. AGNs [9–13]).

Months or years before merging in the LIGO/Virgo

band, BH binaries with masses above a few tens M_\odot spiral in the mHz band of the Laser Interferometer Space Antenna (LISA) [32], a gravitational-wave (GW) space-borne experiment scheduled for 2034. Observing the inspiral with LISA would permit estimating the source parameters very precisely [33–35], e.g., the chirp mass and distance to fractional errors $\sim 10^{-4}$ and ~ 0.4 , respectively, the sky position below $\sim 1 \text{ deg}^2$ – and it would allow for predicting the coalescence time within a minute, weeks before the signal is detected from Earth. This would permit alerting electromagnetic telescopes in advance, pointing them at smaller sky regions, and looking for electromagnetic counterparts [33] *coincident* with the coalescence. Moreover, GR extensions typically predict low-frequency corrections to the GW phase, e.g. vacuum dipole emission at -1 post-Newtonian (PN) order, which will be tested to exquisite precision by LISA inspiral observations [36–38].

We argue below that LISA might detect several gas-rich, high-mass BH binaries. Besides observing these sources beforehand and localizing them accurately [39], LISA will also detect the environmental (i.e. non-vacuum [40]) effects in the GW signal, namely gas accretion and DF on the component BHs, the binary’s acceleration around the AGN’s BH, and possibly the Doppler modulation and the lensing/Shapiro time delay from the central BH. These effects may be degenerate with low-frequency tests of GR, but may help localize the source by correlating with AGN catalogs. Henceforth, we use units where $G = c = 1$.

Event rates. Assuming binaries with parameters drawn from the LVC posteriors, Ref. [2] estimates the comoving merger rate of GW190521-like systems as $0.13^{+0.30}_{-0.11} \text{ yr}^{-1} \text{ Gpc}^{-3}$. With the same hypotheses, LISA will observe 1–10 such systems, depending on high-frequency laser noise, mission lifetime, and operation duty cycle, for $z \lesssim 0.5$ (for more details see [39]). However, if GW190521 lies at the low-mass end of a heavy-BH population extending beyond $100M_\odot$, LISA rates would be significantly higher (because in the $(10 - 10^3)M_\odot$ range the LISA horizon distance is $\propto \mathcal{M}^{5/3}$, with \mathcal{M} the source-frame chirp mass [34]). Indeed, conservatively assuming a Salpeter mass function extending to $200M_\odot$, the inferred LVC rate would boost LISA detections by about an order of magnitude (see also [41]).

Detectability of environmental effects. We model accretion from the AGN disk by the Eddington ratio $f_{\text{Edd}} \equiv \dot{m}/\dot{m}_{\text{Edd}}$ between the mass accretion rate \dot{m} of either BH and $\dot{m}_{\text{Edd}} \equiv L_{\text{Edd}}/\eta$, with L_{Edd} the Eddington luminosity and $\eta \approx 0.1$ the radiative efficiency. The mass growth of the BHs, ($i = 1, 2$), is $m_i(t) = m_i(0) \exp(f_{\text{Edd}} t/\tau_S)$, with $\tau_S = 4.5 \times 10^7 \text{ yr}$ the Salpeter time. The phase term in the Fourier-domain GW signal $\tilde{h} \sim |\tilde{h}| e^{i\tilde{\phi}}$ induced by the mass growth can be evaluated in the stationary-phase approximation at leading PN order [42]:

$$\tilde{\phi}_{\text{accretion}} \approx -f_{\text{Edd}} (8\xi + 15) \frac{75 \mathcal{M}}{851 \, 968 \, \tau_S} [\pi f \mathcal{M}(1+z)]^{-13/3}, \quad (1)$$

with f the observed GW frequency, z the redshift at

coalescence, and $\xi \sim \mathcal{O}(1)$ a factor parameterizing the drag produced by momentum transfer from the accreted gas [42], which we conservatively set to zero.

The binary’s center of mass (CoM) acceleration around the central massive BH also modifies the waveform (c.f. [43–45] for CoM accelerations almost constant during the observation period). The phase correction reads [43–45]

$$\tilde{\phi}_{\text{acceleration}} \approx \frac{25 \mathcal{M}}{65 \, 536} \dot{v}^{\parallel}(t_c) [\pi f \mathcal{M}(1+z)]^{-13/3}, \quad (2)$$

where \dot{v}^{\parallel} is the acceleration along the line of sight, computed at coalescence, dominating over the cosmological acceleration (which we neglect). For quasicircular galactocentric orbits, $\dot{v}^{\parallel} \approx (3.2 \times 10^{-11} \text{ m/s}^2) \epsilon$, where [43]

$$\epsilon = \left(\frac{v_{\text{orb}}}{100 \text{ km/s}} \right)^2 \frac{10 \text{ kpc}}{a} \cos \psi, \quad (3)$$

with v_{orb} the galactocentric orbital velocity, and ψ the angle between line of sight and acceleration. Since $\cos \psi = \cos \iota \sin(\Omega t + \phi_0)$ (with ι the inclination angle of the line of sight relative to the AGN disk, $\Omega = \sqrt{M/a^3}$, and ϕ_0 the initial phase), the assumption of constant acceleration only holds at sufficiently large galactocentric distances a (i.e. low Ω). We will verify this assumption *a posteriori* (and relax it) later.

Eqs. (1)–(2) show that accretion and (constant) acceleration are degenerate, since they both appear at -4 PN order [40, 42, 43, 46] (accretion always yields a negative phase contribution, while acceleration can give contributions of either sign). Both effects can be included in the waveform via a phenomenological PN term $\tilde{\phi}_{-4\text{PN}} = \varphi_{-4} [\pi f \mathcal{M}(1+z)]^{-13/3}$ [47], with φ_{-4} related to f_{Edd} and ϵ for accretion and acceleration, respectively.

We also consider the DF from gas with density ρ surrounding the binary. Assuming a binary’s CoM approximately comoving with the gas, the DF exerts a drag force on each BH (opposite to the BH’s velocity \vec{v}_i in the CoM frame), $F_{\text{DF},i} = 4\pi\rho(Gm_i)^2 I(r_i, v_i)/v_i^2$, where r_i is the distance of the BH from the CoM, and we assume $v_i \gg c_s$ (with c_s the sound speed; note that v_i is relativistic for binaries in the LISA band). We use the analytic ‘‘Coulomb logarithm’’ $I(r, v)$ of [48], which was validated against simulations for $v_i/c_s \lesssim 8$, but which we extrapolate further (c.f. [49]).

We assume $c_s \approx v_{\text{orb}}(H/a)$ [50], with $H/a \sim 0.01$ [27]. Following [48] (see also [51–53]), we only include the effect of the wake created by each BH on itself, and neglect the companion’s [54]. For $f \lesssim 0.3 \text{ Hz}$ this is a good approximation, since the orbital separation of GW190521 in the LISA band is larger than the wake’s size. In the adiabatic approximation, the DF-induced phase correction first enters at -5.5 PN order:

$$\tilde{\phi}_{\text{DF}} \approx -\rho \frac{25\pi(3\nu - 1)\mathcal{M}^2}{739 \, 328 \, v^2} \gamma_{\text{DF}} [\pi f \mathcal{M}(1+z)]^{-16/3}, \quad (4)$$

with $\gamma_{\text{DF}} = -247 \log(f/f_{\text{DF}}) - 39 + 304 \log(20) + 38 \log(3125/8)$ and $f_{\text{DF}} = c_s/[22\pi(m_1 + m_2)]$, being $\nu = m_1 m_2/(m_1 + m_2)^2$ the symmetric mass ratio.

In Fig. 1, we show the distribution of errors – produced with the augmented Fisher formalism of [35] – for the Eddington rate f_{Edd} , the acceleration parameter ϵ , and the gas density ρ , (normalized to $\rho_0 = 10^{-10} \text{ g cm}^{-3}$ [27]), considering modifications one by one. We use $f_{\text{Edd}} = \rho = \epsilon = 0$ as injections, i.e. the distributions represent optimistic upper bounds on the parameters. We use the LVC masses, spins, distance and inclination samples for the NRSur7dq4 model [55] and, for each sample, we set the time to coalescence to the mission’s duration (6 years) and draw sky location and polarization randomly. The extra terms of Eqs. (1), (2), and (4) were added to PhenomD waveforms [56, 57] one by one, and we accounted for the antenna motion during observations following [35, 58, 59]. We consider detections by LISA alone, and jointly with

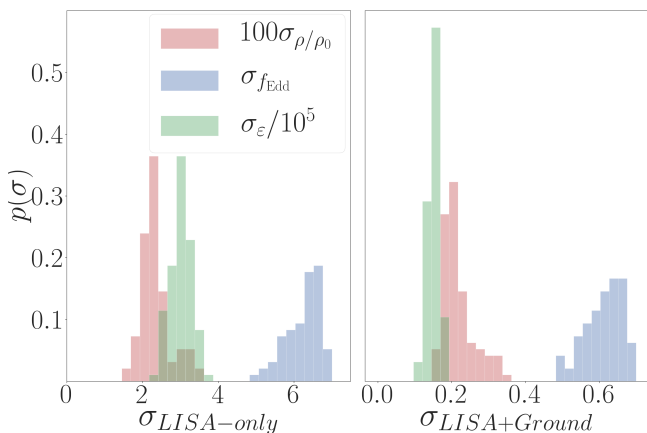


FIG. 1. Distribution of Fisher-matrix errors on environmental effects for the LVC samples with LISA alone or jointly with ground detectors.

ground interferometers. In the *LISA+Ground* case, we mimic a multiband detection by assuming that masses, spins, and merger time are measured by ground detectors, thus removing them from the analysis.

We find that LISA alone can detect super-Eddington accretion rates ($f_{\text{Edd}} \gtrsim 6$), which may be typical in dense environments [60], and acceleration parameters $\epsilon \gtrsim 3 \times 10^5$, corresponding to $a \approx 1 \text{ pc}$ for $M = 10^8 M_\odot$. The DF effect is even stronger, with ρ/ρ_0 constrained at percent level. All errors improve by about an order of magnitude in the *LISA+Ground* scenario (e.g., sub-Eddington accretion rates become measurable).

Next, we focus on one system compatible with the LVC posteriors and perform a Markov-Chain-Monte-Carlo analysis [61] like in [35], injecting nonzero values (plausible for sources in AGNs) for all environmental effects (considered simultaneously): $f_{\text{Edd}} = 5$, $\epsilon = 3.2 \times 10^6$ (corresponding to $a \approx 0.4 \text{ pc}$ for $M = 10^8 M_\odot$) and $\rho = \rho_0$. Fig. 2 shows the posterior distributions for the density (ρ/ρ_0) and the parameter φ_{-4} accounting for acceleration and accretion. Both parameters can be measured well, since they appear at different (negative) PN orders. Note that the sign of φ_{-4} can

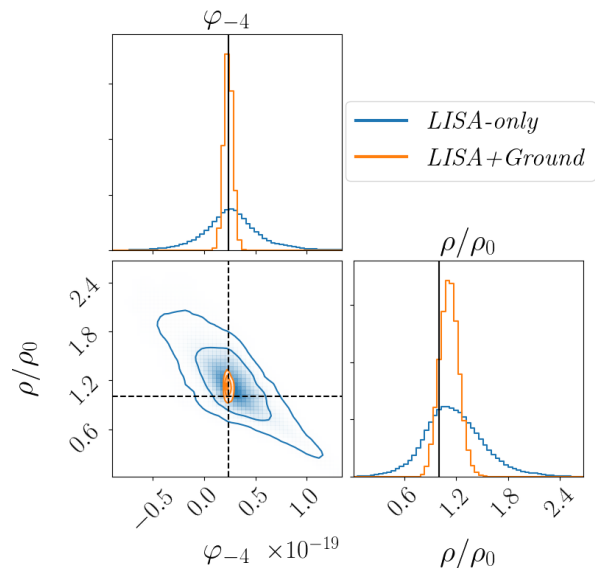


FIG. 2. Posterior distribution of gas density and -4PN phase term (i.e. constant acceleration and/or accretion), with 68%, 95% and 99% confidence contours for a best-case event consistent with GW190521. Black lines indicate the injected values.

help distinguish accretion ($\varphi_{-4} < 0$) from acceleration (φ_{-4} of either sign). We focus on a system with a (LISA-only) signal-to-noise ratio (SNR) of 9.6, the highest among the LVC events, at a distance $\sim 1.4 \text{ Gpc}$. Since this system is close to the LISA detection threshold (SNR ~ 8), we conclude that even for near-threshold events environmental effects are measurable, and their observation will only be limited by the event detectability.

We have checked that the assumption of constant acceleration holds, i.e. verified that the systematic error produced by the variation of ϵ over the observation time T_{obs} is negligible relative to the statistical error. For $a \lesssim 0.25 \text{ pc} [M/(10^8 M_\odot)]^{3/7} [T_{\text{obs}}/(6\text{yr})]^{2/7}$ (i.e. orbital periods $T \lesssim 1200 \text{ yr} [M/(10^8 M_\odot)]^{1/7} [T_{\text{obs}}/(6\text{yr})]^{3/7}$), however, this may no longer be true. This is the case, e.g., if GW190521 lies in a disk migration trap. Ref. [27] estimates the trap’s distance from the central BH as $a \sim 700M$, corresponding to $T \sim 1.8 \text{ yr}$, i.e. the acceleration cannot be assumed constant over the observation time. In this situation, the Taylor expansion leading to Eq. (2) breaks down, and the GW signal can be estimated as $s(t) = h(t + d''(t))$, with $h(t)$ the source-frame strain. The delay $d''(t)$ arises from the change in the source distance due to the orbital motion, and is given by the orbit’s projection on the line of sight: $d''(t) = a \cos \iota \sin(\Omega t + \phi_0)$. This time-varying delay produces an oscillating Doppler modulation $\phi_{\text{Doppler}} \sim 2\pi f d''$ of the observed signal. The magnitude of this phase is approximately

$$2\pi f a \sim 2 \times 10^4 \text{ rad} \left(\frac{M}{10^8 M_\odot} \right) \left(\frac{f}{10 \text{ mHz}} \right) \left(\frac{a}{700M} \right). \quad (5)$$

This effect strongly impacts the signal, dominating the

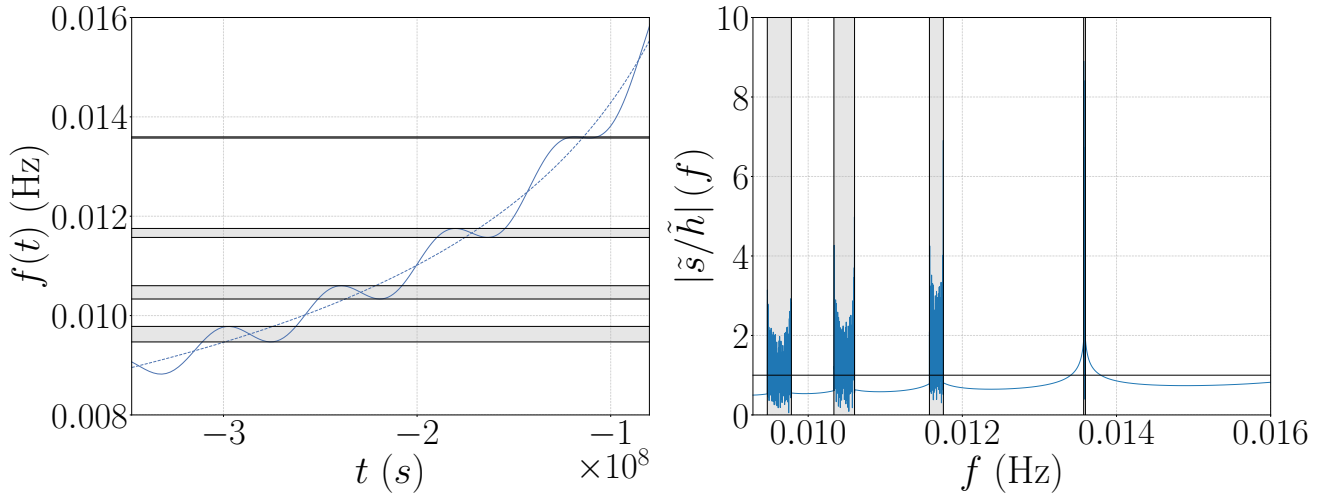


FIG. 3. Doppler modulations of the GW signal due to the motion around the central BH. The left panel shows the time-frequency track of the modulated signal (solid line) compared to the nonmodulated one (dashed) (coalescence is at $t = 0$). The right panel shows the amplitude of the Fourier-domain transfer function $|\tilde{s}/\tilde{h}|(f)$, with a horizontal line at 1. In both panels, the shaded bands show the frequency bands where the time-to-frequency map becomes multivalued.

Doppler modulation produced by the LISA motion (≈ 30 rad), and happening on comparable timescales. The GW frequency suffers redshifts or blueshifts as the binary's CoM moves away from or toward LISA; see Fig. 3. These modulations dominate the GW-driven chirp rate, leading to a multivalued time-to-frequency map in the shaded bands of Fig. 3, where the chirping and anti-chirping parts of the signal overlap. This strongly affects the Fourier-domain observed signal $\tilde{s}(f)$, with the transfer function amplitude $|\mathcal{T}(f)| = |\tilde{s}(f)/\tilde{h}(f)|$ showing interference patterns in the shaded bands. The impact on detection and parameter estimation is under study [39].

Another potentially detectable effect, particularly for edge-on AGN disks, is the strong lensing of the GWs by the central BH, which occurs at scales given by the Einstein radius

$$r_E \simeq (4MD_A)^{1/2} = [4Ma \cos t \sin(\Omega t + \phi_0)]^{1/2}, \quad (6)$$

where we assume $a \ll D_A$, with D_A the lens angular diameter distance. Significant lensing occurs when the source passes within $\sim r_E$ of the lens, and the lensing probability is thus the fraction of time (during a full orbit around the central BH) for which this happens [62, 63]. A GW190521-like event in an AGN disk's migration trap falls either in the repeating-lens regime or in the slowly moving lens regime defined e.g. in [63], depending on the observation time T_{obs} and M . The probability of strong lensing is (see Fig. 4)

$$P_{\text{lens}} = \text{Min} \left[\frac{10^{12} T_{\text{obs}}}{2 \text{ yr}} \left(\frac{a}{M} \right)^{-3/2} \frac{M_{\odot}}{M}, 1 \right] \frac{2}{\pi} \arcsin \left[2 \sqrt{\frac{M}{a}} \right]. \quad (7)$$

Strong lensing also affects the observed waveform directly. For a plane wave, the lensed signal (in real space) is given by

$$h^L(t) = F(f, t) h(t), \quad (8)$$

in terms of the amplification factor $F(f, t)$. For a pointlike lens in the geometric-optics approximation [64, 65],

$$F(f, t) = |\mu_+|^{1/2} - i|\mu_-|^{1/2} e^{2\pi i f \Delta t}, \quad (9)$$

where the magnification of each image, $\mu_{\pm} = 1/2 \pm (y^2 + 2)/(2y\sqrt{y^2 + 4})$, depends on time through the lensing parameter $y \equiv b/r_E$, with b the impact parameter. The time delay between two images is $\Delta t = \Delta t_{\text{fid}} [y/2\sqrt{y^2 + 4} + \ln((\sqrt{y^2 + 4} + y)/(\sqrt{y^2 + 4} - y))]$ where $\Delta t_{\text{fid}} \simeq 2 \times 10^{-5} (1 + z) M/M_{\odot} \text{sec}$. Periodic passages of the orbit behind the central massive BH will produce repeated interference patterns on the observed waveform. From Eq. (8), one sees that besides rescaling the waveform amplitude, strong lensing also yields an additive correction to the phase. For a plane wave, the latter is simply $\phi_{\text{SL}} = \text{Arg}[F(f, t)]$. We have checked, however, that this dephasing is typically smaller than the Doppler modulation described above (c.f. [39] for details).

Discussion. If GW190521-like events occur in dense gaseous environments, these GW sources may provide a unique probe of AGN properties. By detecting the inspiral of these binaries months or years before their coalescence in the band of ground-based detectors [39], LISA will measure the binary parameters with exquisite precision and help localize potential electromagnetic counterparts (which would in turn help identify the host galaxy among the thousands – of which just a few AGNs – present within the 1 deg^2 LISA error-box). Moreover, LISA may uncover nonvacuum effects carrying information on the astrophysical source environment, further confirming the identification with an electromagnetic counterpart (if any).

Detecting environmental effects is also crucial to test GR [40]. Effects like extra dimensions or a time-varying Newton constant enter the inspiral waveform at

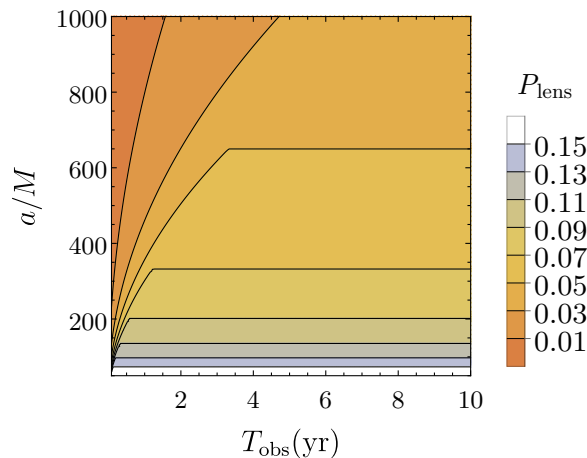


FIG. 4. Lensing probability as function of observation time, T_{obs} , and galactocentric distance, a/M , for $M = 10^8 M_{\odot}$.

–4PN order [66], being thus degenerate with accretion or acceleration. Other effects, like vacuum dipole emission, also appear at negative PN orders [36]. If negative PN corrections are measured by standard parameterized tests [47], an electromagnetic counterpart in the LISA sky-position error box would favor an environmental origin over a beyond-GR one.

Given these tantalizing prospects, dedicated simulations would be needed to carefully describe environmental effects in binaries, accounting e.g. for radiative transfer and outflows that may affect DF and accretion [60, 67], and modeling strong accelerations in relativistic binaries accurately [39]. Relativistic corrections might also impact the signal, if the binary is close to the central BH (note that $a \approx 700M$ corresponds to $v_{\text{orb}} \approx 0.04$). These include orbital periastron precession, spin-orbit [68] and spin-spin [69] precession, and gravitational redshift. The Shapiro time delay can also be significant, i.e. $\delta t \sim 10^3 \text{ s} \left(\frac{M}{10^8 M_{\odot}} \right)$ as we will discuss in [39]. The central BH may also produce Lidov-Kozai oscillations, increasing the binary’s eccentricity [70, 71].

Besides the merger remnant’s emission in optical, X-rays from accretion onto the binary components and radio flares from jets are expected. Following [42], we find both effects difficult to observe even with future telescopes (e.g. Athena+, Square Kilometer Array) [39].

Acknowledgments. We acknowledge financial support from the European Union’s H2020 ERC Consolidator Grants “GRavity from Astrophysical to Microscopic Scales”, grant agreement no. GRAMS-815673 (to E.B.), and “Binary Massive Black Hole Astrophysics”, grant agreement no. BMassive-818691 (to A.S.); from the Swiss National Science Foundation; from the French space agency CNES in the framework of the LISA mission; from the European Union’s H2020 ERC, Starting Grant agreement no. DarkGRA–757480 (to P.P.); from the MIUR PRIN and FARE programmes (GW-NEXT, CUP: B84I20000100001, to P.P.). We thank I. Bartos,

J.-M. Ezquiaga, J. Calderon Bustillo, and especially T. Dal Canton for insightful comments.

- [1] R. Abbott *et al.* (LIGO Scientific, Virgo), *Phys. Rev. Lett.* **125**, 101102 (2020), arXiv:2009.01075 [gr-qc].
- [2] R. Abbott *et al.* (LIGO Scientific, Virgo), *Astrophys. J. Lett.* **900**, L13 (2020), arXiv:2009.01190 [astro-ph.HE].
- [3] S. E. Woosley, A. Heger, and T. A. Weaver, *Reviews of Modern Physics* **74**, 1015 (2002).
- [4] A. Heger, C. L. Fryer, S. E. Woosley, N. Langer, and D. H. Hartmann, *The Astrophysical Journal* **591**, 288 (2003), arXiv:astro-ph/0212469 [astro-ph].
- [5] R. Farmer, M. Renzo, S. E. de Mink, P. Marchant, and S. Justham, *The Astrophysical Journal* **887**, 53 (2019), arXiv:1910.12874 [astro-ph.SR].
- [6] D. Gerosa and E. Berti, *Phys. Rev. D* **95**, 124046 (2017), arXiv:1703.06223 [gr-qc].
- [7] C. L. Rodriguez, M. Zevin, P. Amaro-Seoane, S. Chatterjee, K. Kremer, F. A. Rasio, and C. S. Ye, *Phys. Rev. D* **100**, 043027 (2019), arXiv:1906.10260 [astro-ph.HE].
- [8] G. Fragione, A. Loeb, and F. A. Rasio, arXiv e-prints, arXiv:2009.05065 (2020), arXiv:2009.05065 [astro-ph.GA].
- [9] Y. Levin, *Mon. Not. R. Astron. Soc.* **374**, 515 (2007), arXiv:astro-ph/0603583 [astro-ph].
- [10] B. McKernan, K. E. S. Ford, R. O’Shaughnessy, and D. Wysocki, *Mon. Not. R. Astron. Soc.* **494**, 1203 (2020), arXiv:1907.04356 [astro-ph.HE].
- [11] H. Tagawa, Z. Haiman, and B. Kocsis, *The Astrophysical Journal* **898**, 25 (2020), arXiv:1912.08218 [astro-ph.GA].
- [12] I. Bartos, B. Kocsis, Z. Haiman, and S. Márka, *Astrophys. J.* **835**, 165 (2017), arXiv:1602.03831 [astro-ph.HE].
- [13] Y. Yang, I. Bartos, Z. Haiman, B. Kocsis, Z. Marka, N. Stone, and S. Marka, *Astrophys. J.* **876**, 122 (2019), arXiv:1903.01405 [astro-ph.HE].
- [14] T. Kinugawa, T. Nakamura, and H. Nakano, (2020), arXiv:2009.06922 [astro-ph.HE].
- [15] T. Kinugawa, T. Nakamura, and H. Nakano, *Mon. Not. Roy. Astron. Soc.* **498**, 3946 (2020), arXiv:2005.09795 [astro-ph.HE].
- [16] M. Safarzadeh and Z. Haiman, (2020), arXiv:2009.09320 [astro-ph.HE].
- [17] E. J. Farrell, J. H. Groh, R. Hirschi, L. Murphy, E. Kaiser, S. Ekström, C. Georgy, and G. Meynet, (2020), arXiv:2009.06585 [astro-ph.SR].
- [18] J. Sakstein, D. Croon, S. D. McDermott, M. C. Straight, and E. J. Baxter, (2020), arXiv:2009.01213 [gr-qc].
- [19] V. De Luca, V. Desjacques, G. Franciolini, P. Pani, and A. Riotto, (2020), arXiv:2009.01728 [astro-ph.CO].
- [20] J. Calderón Bustillo, N. Sanchis-Gual, A. Torres-Forné, J. A. Font, A. Vajpeyi, R. Smith, C. Herdeiro, E. Radu, and S. H. W. Leong, arXiv e-prints, arXiv:2009.05376 (2020), arXiv:2009.05376 [gr-qc].
- [21] J. W. Moffat, arXiv e-prints, arXiv:2009.04360 (2020), arXiv:2009.04360 [gr-qc].
- [22] M. Fishbach and D. E. Holz, arXiv e-prints, arXiv:2009.05472 (2020), arXiv:2009.05472 [astro-ph.HE].
- [23] A. H. Nitz and C. D. Capano, (2020), arXiv:2010.12558 [astro-ph.HE].
- [24] V. Gayathri, J. Healy, J. Lange, B. O’Brien, M. Szczepanczyk, I. Bartos, M. Campanelli, S. Klimentko, C. Lousto, and

- R. O’Shaughnessy, arXiv e-prints , arXiv:2009.05461 (2020), arXiv:2009.05461 [astro-ph.HE].
- [25] I. M. Romero-Shaw, P. D. Lasky, E. Thrane, and J. Calderon Bustillo, arXiv e-prints , arXiv:2009.04771 (2020), arXiv:2009.04771 [astro-ph.HE].
- [26] J. Calderón Bustillo, N. Sanchis-Gual, A. Torres-Forné, and J. A. Font, (2020), arXiv:2009.01066 [gr-qc].
- [27] M. J. Graham, K. E. S. Ford, B. McKernan, N. P. Ross, D. Stern, K. Burdge, *et al.*, *Phys. Rev. Lett.* **124**, 251102 (2020).
- [28] V. Connaughton *et al.*, *Astrophys. J. Lett.* **826**, L6 (2016), arXiv:1602.03920 [astro-ph.HE].
- [29] V. Savchenko *et al.*, *Astrophys. J. Lett.* **820**, L36 (2016), arXiv:1602.04180 [astro-ph.HE].
- [30] J. M. Bellovary, M.-M. Mac Low, B. McKernan, and K. E. S. Ford, *The Astrophysical Journal* **819**, L17 (2016), arXiv:1511.00005 [astro-ph.GA].
- [31] G. Ashton, K. Ackley, I. M. n. Hernandez, and B. Piotrkowski, (2020), arXiv:2009.12346 [astro-ph.HE].
- [32] P. Amaro-Seoane *et al.* (LISA), (2017), arXiv:1702.00786 [astro-ph.IM].
- [33] A. Sesana, *Phys. Rev. Lett.* **116**, 231102 (2016), arXiv:1602.06951 [gr-qc].
- [34] K. Jani, D. Shoemaker, and C. Cutler, *Nature Astronomy* **4**, 260 (2019), arXiv:1908.04985 [gr-qc].
- [35] A. Toubiana, S. Marsat, S. Babak, J. Baker, and T. Dal Canton, (2020), arXiv:2007.08544 [gr-qc].
- [36] E. Barausse, N. Yunes, and K. Chamberlain, *Phys. Rev. Lett.* **116**, 241104 (2016), arXiv:1603.04075 [gr-qc].
- [37] S. Vitale, *Physical Review Letters* **117** (2016), 10.1103/physrevlett.117.051102.
- [38] A. Toubiana, S. Marsat, S. Babak, E. Barausse, and J. Baker, *Phys. Rev. D* **101**, 104038 (2020), arXiv:2004.03626 [gr-qc].
- [39] A. Toubiana *et al.*, (In preparation).
- [40] E. Barausse, V. Cardoso, and P. Pani, *Phys. Rev. D* **89**, 104059 (2014), arXiv:1404.7149 [gr-qc].
- [41] J. M. Ezquiaga and D. E. Holz, (2020), arXiv:2006.02211 [astro-ph.HE].
- [42] A. Caputo, L. Sberna, A. Toubiana, S. Babak, E. Barausse, S. Marsat, and P. Pani, *Astrophys. J.* **892**, 90 (2020), arXiv:2001.03620 [astro-ph.HE].
- [43] C. Bonvin, C. Caprini, R. Sturani, and N. Tamanini, *Phys. Rev. D* **95**, 044029 (2017), arXiv:1609.08093 [astro-ph.CO].
- [44] K. Inayoshi, N. Tamanini, C. Caprini, and Z. Haiman, *Phys. Rev. D* **96**, 063014 (2017), arXiv:1702.06529 [astro-ph.HE].
- [45] N. Tamanini, A. Klein, C. Bonvin, E. Barausse, and C. Caprini, *Phys. Rev. D* **101**, 063002 (2020), arXiv:1907.02018 [astro-ph.IM].
- [46] V. Cardoso and A. Maselli, (2019), arXiv:1909.05870 [astro-ph.HE].
- [47] B. Abbott *et al.* (LIGO Scientific, Virgo), *Phys. Rev. Lett.* **116**, 221101 (2016), [Erratum: *Phys. Rev. Lett.* **121**, 129902 (2018)], arXiv:1602.03841 [gr-qc].
- [48] H. Kim and W.-T. Kim, *Astrophys. J.* **665**, 432 (2007), arXiv:0705.0084 [astro-ph].
- [49] B. Kocsis, N. Yunes, and A. Loeb, *Phys. Rev. D* **84**, 024032 (2011), arXiv:1104.2322 [astro-ph.GA].
- [50] J. Frank, A. King, and D. J. Raine, *Accretion Power in Astrophysics, by Juhan Frank and Andrew King and Derek Raine, pp. 398. ISBN 0521620538. Cambridge, UK: Cambridge University Press, February 2002.* (2002) p. 398.
- [51] E. C. Ostriker, *Astrophys. J.* **513**, 252 (1999), arXiv:astro-ph/9810324 [astro-ph].
- [52] E. Barausse, *Mon. Not. Roy. Astron. Soc.* **382**, 826 (2007), arXiv:0709.0211 [astro-ph].
- [53] C. F. Macedo, P. Pani, V. Cardoso, and L. C. Crispino, *Astrophys. J.* **774**, 48 (2013), arXiv:1302.2646 [gr-qc].
- [54] H. Kim, W.-T. Kim, and F. J. Sanchez-Salcedo, *Astrophys. J.* **679**, L33 (2008), arXiv:0804.2010 [astro-ph].
- [55] V. Varma, S. E. Field, M. A. Scheel, J. Blackman, D. Gerosa, L. C. Stein, L. E. Kidder, and H. P. Pfeiffer, *Phys. Rev. Research.* **1**, 033015 (2019), arXiv:1905.09300 [gr-qc].
- [56] S. Husa, S. Khan, M. Hannam, M. Pürrer, F. Ohme, X. J. Forteza, and A. Bohé, *Phys. Rev. D* **93**, 044006 (2016).
- [57] S. Khan, S. Husa, M. Hannam, F. Ohme, M. Pürrer, X. J. Forteza, and A. Bohé, *Phys. Rev. D* **93**, 044007 (2016).
- [58] S. Marsat and J. G. Baker, (2018), arXiv:1806.10734 [gr-qc].
- [59] S. Marsat, J. G. Baker, and T. Dal Canton, (2020), arXiv:2003.00357 [gr-qc].
- [60] X. Li, P. Chang, Y. Levin, C. D. Matzner, and P. J. Armitage, *Mon. Not. Roy. Astron. Soc.* **494**, 2327 (2020), arXiv:1912.06864 [astro-ph.HE].
- [61] R. L. Karandikar, *Sadhana* **31**, 81 (2006).
- [62] D. J. D’Orazio and A. Loeb, *Phys. Rev. D* **101**, 083031 (2020), arXiv:1910.02966 [astro-ph.HE].
- [63] D. J. D’Orazio and R. Di Stefano, *Mon. Not. Roy. Astron. Soc.* **474**, 2975 (2018), arXiv:1707.02335 [astro-ph.HE].
- [64] P. Schneider, J. Ehlers, and E. E. Falco, *Gravitational Lenses* (Springer Verlag, 1992).
- [65] R. Takahashi and T. Nakamura, *Astrophys. J.* **595**, 1039 (2003), arXiv:astro-ph/0305055.
- [66] N. Yunes, K. Yagi, and F. Pretorius, *Phys. Rev. D* **94**, 084002 (2016), arXiv:1603.08955 [gr-qc].
- [67] A. Gruzinov, Y. Levin, and C. D. Matzner, (2019), arXiv:1906.01186 [astro-ph.HE].
- [68] H. Yu and Y. Chen, (2020), arXiv:2009.02579 [gr-qc].
- [69] Y. Fang, X. Chen, and Q.-G. Huang, *The Astrophysical Journal* **887**, 210 (2019), arXiv:1908.01443 [astro-ph.HE].
- [70] M. L. Lidov, *Planet. Space Sci.* **9**, 719 (1962).
- [71] Y. Kozai, *Astron. J.* **67**, 591 (1962).